

# Upscaling leaf area index in an Arctic landscape through multiscale observations

M. WILLIAMS\*, R. BELL\*, L. SPADAVECCHIA\*, L. E. STREET\* and M. T. VAN WIJK†

\*School of GeoSciences and NERC Centre for Terrestrial Carbon Dynamics, University of Edinburgh, Edinburgh EH9 3JN, UK,

†Plant Production Systems, Wageningen University, Plant Sciences, Haarweg 333, 6709 RZ Wageningen, The Netherlands

## Abstract

Monitoring and understanding global change requires a detailed focus on upscaling, the process for extrapolating from the site-specific scale to the smallest scale resolved in regional or global models or earth observing systems. Leaf area index (LAI) is one of the most sensitive determinants of plant production and can vary by an order of magnitude over short distances. The landscape distribution of LAI is generally determined by remote sensing of surface reflectance (e.g. normalized difference vegetation index, NDVI) but the mismatch in scales between ground and satellite measurements complicates LAI upscaling. Here, we describe a series of measurements to quantify the spatial distribution of LAI in a sub-Arctic landscape and then describe the upscaling process and its associated errors. Working from a fine-scale harvest LAI–NDVI relationship, we collected NDVI data over a 500 m × 500 m catchment in the Swedish Arctic, at resolutions from 0.2 to 9.0 m in a nested sampling design. NDVI scaled linearly, so that NDVI at any scale was a simple average of multiple NDVI measurements taken at finer scales. The LAI–NDVI relationship was scale invariant from 1.5 to 9.0 m resolution. Thus, a single exponential LAI–NDVI relationship was valid at all these scales, with similar prediction errors. Vegetation patches were of a scale of ~0.5 m and at measurement scales coarser than this, there was a sharp drop in LAI variance. Landsat NDVI data for the study catchment correlated significantly, but poorly, with ground-based measurements. A variety of techniques were used to construct LAI maps, including interpolation by inverse distance weighting, ordinary Kriging, External Drift Kriging using Landsat data, and direct estimation from a Landsat NDVI–LAI calibration. All methods produced similar LAI estimates and overall errors. However, Kriging approaches also generated maps of LAI estimation error based on semivariograms. The spatial variability of this Arctic landscape was such that local measurements assimilated by Kriging approaches had a limited spatial influence. Over scales > 50 m, interpolation error was of similar magnitude to the error in the Landsat NDVI calibration. The characterisation of LAI spatial error in this study is a key step towards developing spatio-temporal data assimilation systems for assessing C cycling in terrestrial ecosystems by combining models with field and remotely sensed data.

*Keywords:* Arctic, data assimilation, geostatistics, Kriging, LAI, Landsat, NDVI, remote sensing, semivariogram, tundra

*Received 10 September 2007; revised version received 14 December 2007 and accepted 14 December 2007*

## Introduction

Leaf area index (LAI) is a vegetation characteristic with a dominant role in controlling primary production, evapotranspiration, surface energy balance, and biogeochemical cycling. LAI is thus a critical part of many

global change studies, including those focussing on identifying recent changes in plant growth (Myneni *et al.*, 1997; Jia *et al.*, 2006) or interpreting measurements of net carbon fluxes from global networks (Owen *et al.*, 2007). LAI is also a key variable in vegetation/biogeochemical models (Sitch *et al.*, 2003) and land surface schemes in general circulation models (Essery *et al.*, 2001), and its variation across space must be determined to improve model predictions.

Correspondence: M. Williams, e-mail: mat.williams@ed.ac.uk

Leaf area index can be highly heterogeneous. For instance, LAI in Arctic ecosystems can vary by an order of magnitude over landscapes (Williams & Rastetter, 1999) due to the patchiness of vegetation. The size of vegetation patches, and the range and statistical distribution of LAI in the landscape, are generally poorly recorded worldwide. The patchiness of ecosystem structure and function thus represents a major challenge in upscaling LAI (Williams *et al.*, 2001; Boelman *et al.*, 2005). In the Arctic, changes in LAI are already occurring, resulting in feedbacks to regional climate (Chapin *et al.*, 2005).

Upscaling can be defined as the process for extrapolating from the site-specific scale, at which direct observations are made, to the smallest scale resolved in regional or global models or earth observing systems (Harvey, 2000). Because the terrestrial biosphere is characterized by spatial heterogeneity and non-linear processes, it is important to determine whether the relationships determined at fine scales in field research are applicable directly at coarser scales. Without proper care, significant errors can be introduced in the upscaling process.

Because LAI is related to the surface energy balance, satellite and airborne instruments provide a means to monitor LAI remotely (Tian *et al.*, 2002). Remote sensing does not, however, measure LAI directly. Observations of surface reflectance, often the normalized difference vegetation index (NDVI), the normalized ratio between the red and infrared bands, are generally calibrated against direct observations of LAI from field measurements (Boelman *et al.*, 2003; Van Wijk & Williams, 2005). A particular source of error is caused by differences in spatial scale between remote observations and direct measurements (Woodcock & Strahler, 1987). Williams *et al.* (2001) showed a poor correlation between LAI measured in destructive harvests in Arctic tundra in  $0.2\text{ m} \times 0.2\text{ m}$  quadrats vs. NDVI data from satellites at  $1\text{ km}^2$  resolution.

Here, we describe a series of measurements to map and quantify the spatial distribution of LAI in a sub-Arctic landscape. Our overall objective is to test an upscaling approach so that uncertainty in landscape LAI can be directly determined. The landscape scale selected ( $500\text{ m} \times 500\text{ m}$ ) is highly relevant as it represents the approximate scale of sampling by eddy flux instrumentation used to monitor C fluxes, and it also spans the scale of key earth observation sensors, such as Landsat ETM+ and MODIS. With a detailed knowledge of LAI at this scale, it should be possible to interpret flux data and satellite information more effectively for global change research.

In a microscale study (spatial resolutions from 0.2 to 9.0 m), determinations of LAI from harvests were linked

to a series of scaled observations of NDVI collected with handheld instruments. We tested the hypothesis (H1) that NDVI averaged linearly at resolutions from 0.2 to 9.0 m. If proven, this relationship simplifies upscaling. We then tested the hypothesis (H2) that LAI–NDVI relationships were scale-invariant. Scale-invariance means that an NDVI–LAI relationship developed at a fine scale can be applied at a coarser scale. We hypothesized (H3) that the range of LAI data estimated for a sample area would increase at finer sensor resolutions. We expected that the distribution of estimated LAI would be increasingly skewed at finer resolutions, because much of the Arctic land surface has low LAI values and is patchy at fine scales (Williams & Rastetter, 1999; Street *et al.*, 2007). Any shift in the distribution of estimated LAI will have important implications for any process non-linearly associated with LAI.

We then determined the capacity of satellite remote sensing approaches to retrieve information on spatial distribution of LAI. In a macroscale study (spatial resolutions from 10 to 500 m) overlaid on the microscale measurement area, we compared collocated ground-based estimates of NDVI (9 m resolution) to satellite data (30 m resolution). Our first objective was to test the quality of space-borne observations of NDVI. Our second objective was to construct maps of LAI using a variety of methods, including interpolation of ground data, direct application of calibrated remotely sensed data, and a combination of the two. We hypothesized (H4) that geostatistical interpolations of ground data combined through Kriging with remotely sensed NDVI data, would produce better maps than either interpolation or satellite-based approaches alone.

There is an increasing interest in data assimilation (DA) approaches (Raupach *et al.*, 2005; Williams *et al.*, 2005) for modelling studies, whereby models and multiple observations are combined to produce an analysis of a system with quantified confidence levels. For regional DA, provision of estimation errors and their spatial structure is vital, so we generated maps of LAI estimation error. We conclude by discussing how studies of this type can guide the process of assimilating remote sensing observations into ecosystem C models.

Previous studies have correlated ground measurements of LAI against satellite NDVI (Turner *et al.*, 1999) in temperate and boreal ecosystems. But these studies have not taken explicit account of the difference in scales between satellite pixels and ground data collections, nor assessed NDVI at ground level for direct comparison to satellite data. Our study is novel in that, for the first time, a nested design has been used to upscale direct, harvest measurements of LAI to the landscape scale, with reflectance measurements employed at all scales from ground to satellite. This

experimental design means it is possible to track the development of errors throughout the upscaling and properly quantify canopy heterogeneity.

## Methods

### The study area

This study was carried out in a 500 m × 500 m area located within the sub-Arctic zone of Fennoscandia, an ecotone between taiga and tundra characterized by deciduous birch forests with low altitudinal tree lines, above which heath and mire communities predominate (Callaghan & Karlsson, 1996). The study area was located above the tree line near Abisko, Sweden (68°18'N, 18°50'E) at an average elevation of 620 m at the centre of a shallow valley draining northwards, hereafter known as the intensive valley (IV). At Abisko, the average rainfall is 400 mm per annum and average temperatures are −1 °C (Anderson *et al.*, 1996). A stream running through the centre of the area was bordered by shrubby riparian vegetation characterized by *Betula nana* and *Salix* species. Elsewhere, vegetation was dominated by a low heath characterized by *Empetrum nigrum*, with *B. nana* growing in more sheltered dips. There were some scattered wooded areas characterized by *Betula pubescens* usually with a *Vaccinium* understory.

### Skye NDVI and LAI measurements

Measurements were carried out at two scales within the IV. The 'microscale' study (testing H1–H3) focussed on detailed measurements within a 40 m × 40 m area straddling the stream and foot-slopes of the IV. The 'macroscale' study (testing H4) involved estimates of NDVI from a 500 m × 500 m area spanning the upper slopes and valley floor of the IV, and including the microscale site at its centre (Fig. 1).

The microscale study involved measurements in nine 10 m × 10 m plots laid out in a regular grid at 5 m spacing in the 40 m × 40 m domain, collected between 10th and 31st July 2002 (Van Wijk & Williams, 2005). In each 10 m × 10 m plot, direct harvest measurements of LAI (harvest LAI) were determined in nine 0.2 m × 0.2 m quadrats (Williams & Rastetter, 1999). A series of indirect LAI measurements were also obtained on each quadrat preharvest using (1) NDVI obtained with a Skye Instruments 2 Channel Sensor SKR1800 (Skye Instruments, Powys, UK; channel 1 = 0.56–0.68 μm, channel 2 = 0.725–1.1 μm) with calibrations traceable to the National Physical Laboratory, UK, and the diffuser off (Skye NDVI), and (2) a LI-COR LAI-2000 Canopy Analyzer (LI-COR, Lincoln, NE, USA), collecting one above- and one below-canopy measurement (LAI-2000

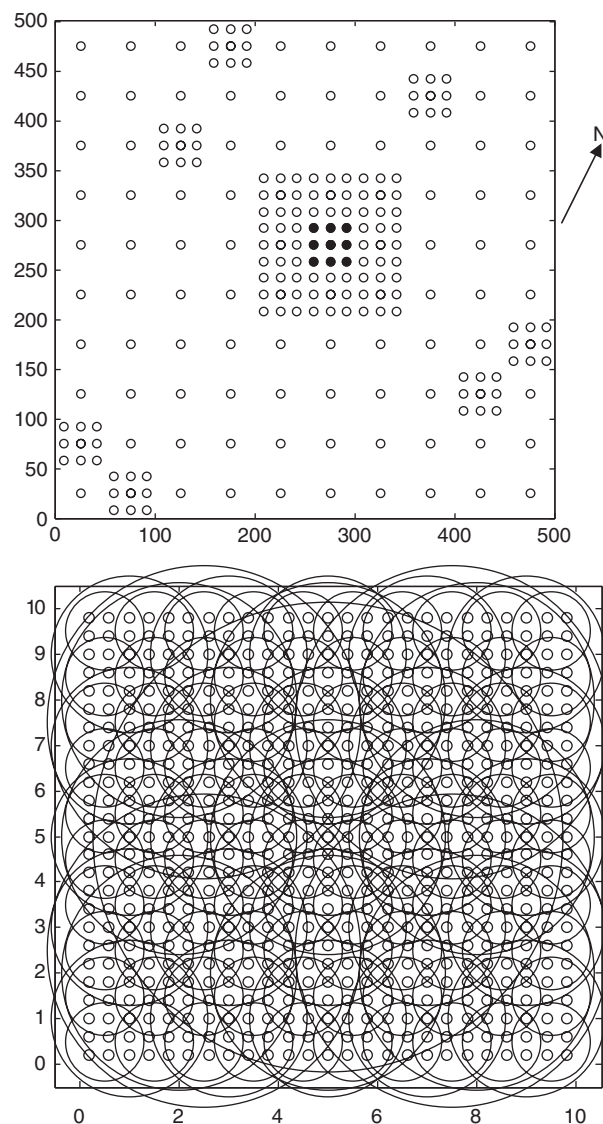


**Fig. 1** Top panel: the 500 m × 500 m macroscale experimental design, and its approximate orientation. Circles: the locations and sampling area of 9 m resolution Skye NDVI observations. Filled circles: the location of the microscale study area. Bottom panel: the nested multiscale experimental design for one of the nine microscale 10 m × 10 m plots. Circles: the locations and approximate sampling area of Skye NDVI, with scales ranging from 0.2 m (smallest circles,  $n = 625$ ) to ~9.0 m (the largest circle,  $n = 1$ ). LAI-2000 data were also collected at the points indicated by the smallest circles. Both figures have scales in metres.

LAI). The harvest LAI data were used to calibrate the indirect sensors; see Van Wijk & Williams (2005) for full details.

The spatial variability of LAI within the nine microscale plots was determined by performing paired LAI-2000 and NDVI measurements, each giving an estimated resolution of 0.2 m, in each plot in a regular

**Table 1** The design of multiscale NDVI measurements on 10 m × 10 m microscale plots

Measurement height (m)	Area measured (m <sup>2</sup> )	Diameter of ground survey (m)	No. of measurements per 10 m × 10 m plot
0.9*	0.03	0.2	525
0.5	1.77	1.5	100
1.0	7.07	3.0	25
1.5	15.9	4.5	9
2.0	28.3	6.0	5
3.0	63.6	9.0	1

Nine 10 m × 10 m plots were sampled in this way.

\*The diffuser was not used, so field of view was reduced.

grid at 0.4 m intervals. Six hundred and twenty-five measurements for each instrument were collected in each plot, giving 5625 measurements at 0.2 m resolution for the microscale study. Harvest LAIs in the microscale study were closely related to Skye NDVI values, but the best estimates of LAI were generated by combining information from co-located LAI-2000 and Skye NDVI data, with parameters estimated by maximum likelihood methods (Van Wijk & Williams, 2005). Besides estimating the NDVI at 0.2 m resolution on a regular grid of 0.4 m, we also estimated the Skye NDVI of larger surface areas on successively coarser grids (Fig. 1). A cosine collecting adapter ('diffuser cap') extended the field-of-view of the Skye sensor to ~113°, and the area of reflectance measurement was further increased by raising the sensor height using light-weight poles. The sensor heights, the area measured, the pixel resolution and the number of measurements taken at coarser scales are shown in Table 1. The experimental design meant that measurements at a coarse resolution could be directly compared with multiple fine resolution data collected within the coarse pixel.

The macroscale study was undertaken between 14th and 25th August 2004. A 500 m × 500 m area was set up centred on the microscale study (Fig. 1). The macroscale area was divided into 100 50 m × 50 m plots on a 10 × 10 grid (Fig. 1). Sixteen of the 50 m × 50 m plots were subdivided into nine 10 m × 10 m intensive plots on a 3 × 3 grid with 5 m spacing to generate a nested sampling design with 228 plots. The central intensive 50 m × 50 m plot corresponded with, and resampled, the microscale study of 2002. At the centre of each plot (whether 50 m × 50 m, or 10 m × 10 m) a Skye NDVI reading was recorded with the sensor suspended 3 m above the ground (Table 1) with a nominal resolution of 9 m. The location of each plot centre was determined using GPS, with spatial error estimated at ~6 m. Some plots had a covering of birch trees (>2 m tall) which

precluded the use of the Skye sensor. These locations ( $n = 31$ ) were excluded from the sampling analysis, so that the focus was purely on tundra vegetation in the remaining 197 macroscale plots.

#### Remote sensing

Remote sensing observations for the Abisko region were generated from Landsat 7 ETM+ data, with a nominal resolution of 30 m, collected from an overpass on 20 August 2001. The image belonged to the NASA's orthorectified dataset and was geo-referenced to a root-mean-square error (RMSE) of 50 m (Tucker *et al.*, 2004). In order to confirm this claim and improve the accuracy, further geo-referencing was carried out using a 1:100 000 scale map belonging to the Lantmäteriet series. Twelve ground control points were used to give an image with a final RMSE of <35 m. We used bands 3 (red, 0.63–0.69 µm) and 4 (near infrared, 0.78–0.90 µm) to determine Landsat NDVI. Landsat NDVI estimates corresponding to each ground measurement were generated by interpolation, using distance weighted averaging (ARC/INFO software, ESRI, Redlands, USA) for each macroscale plot for comparison with Skye NDVI measurements and LAI estimates for these locations. There were no corrections undertaken to the Landsat data to account for atmospheric effects on the data.

Airborne remote sensing was undertaken using a helicopter, with the Skye NDVI sensor mounted externally on a boom. The macroscale area was located from the air using GPS, and the helicopter hovered over the centre of the study area at a height of 235 m above the ground surface. Given the field of view with the cosine adapter, the ground resolution (i.e. diameter) of the single NDVI observation was ~700 m, slightly larger than the domain of ground measurements (500 m).

#### Geospatial methods

To identify the pattern in spatial measurements of the microscale and macroscale areas, and also the remote sensing data, we generated semivariograms, a description of the spatial autocorrelation structure of the data (Cressie, 1993). For a stationary process, there is generally an increase in semivariance with increased separation vector, up to some threshold distance, referred to as the range. At separation distances greater than the range, the semivariance remains at a constant 'sill' value. The semivariance at zero separation is known as the nugget.

We fitted an exponential model of semivariance

$$g(h) = \tau + c \left[ 1 - \exp\left(\frac{-3h}{\phi}\right) \right],$$

where  $\tau$  is the 'nugget' variance,  $c$  is the contribution of the exponential structure, and  $\phi$  is the effective range, interpreted as the distance at which  $g(h)$  reaches 95% of the asymptotic 'sill' variance ( $\tau + c$ ). The factor of 3 in the numerator solves for effective range. The model was fit to the data by minimising the sum of squares differences.

### Generating LAI maps

We used a variety of methods, from relatively simple to more complex, to generate maps of LAI for the macroscale area, using various combinations of ground and satellite observations (Table 2). Inverse distance weighting (IDW) is an interpolation technique that makes use of estimates of LAI, derived from Skye NDVI, and information on their spatial arrangement. LAI values across the macroscale domain were generated through weighted averaging of the 197 macroscale plots, with weights determined according to distance. The Landsat correlation model (LCM) approach used the linear regression of Landsat NDVI (30 m resolution) against ground-based estimates of LAI (9 m resolution, from Skye NDVI data) for the same locations. The linear regression was then used to estimate LAI for all Landsat NDVI pixels over the IV.

Kriging refers to a set of multiple linear regression procedures by which the best linear unbiased estimate of an unobserved datum value is arrived at by the weighted linear combination of surrounding observations, such that the prediction error is minimized (Isaaks & Srivastava, 1990; Goovaerts, 1999). The weights ascribed to each observation are arrived at by taking into consideration the clustering of the data locations (with points from over-sampled locations being down-weighted), and the proximity of each observation to the prediction location. These spatial effects

are included via reference to the autocorrelation structure of the dataset, as summarized by the semivariogram. Ordinary Kriging (OK) involved generating an interpolated LAI map using ground-based LAI data and their semivariograms. An additional output from Kriging is a prediction of interpolation error, provided by the geostatistics of the semivariograms.

More complex spatial regression models partition the spatial information into a largescale trend component, and a stationary, spatially autocorrelated residual component (i.e. nonstationary geostatistics). In External Drift Kriging (EDK), we used a secondary covariate 'external' to the semivariance calculation for our data as extra spatial information (Deutsch & Journel, 1998). Here, we require that the variation of the secondary data, in this case Landsat NVDI data, be smoothly and linearly related to the local variable, the estimates of LAI. The covariates must be sampled at all observation and all prediction locations. The extra covariate informs the interpolation, so that the more spatially complete remote sensing observations improve interpolation skill.

The interpolation skill of each technique was assessed by statistical resampling. The jackknife approach involved systematically recomputing the interpolations, leaving out one observation at a time. The ability of the interpolation routine to predict the missing observations can then be used to construct statistics, such as a RMSE and mean absolute error (MAE).

## Results

### Microscale study

**Microscale NDVI.** The mean microscale site NDVI estimated by averaging  $0.2\text{ m} \times 0.2\text{ m}$  NDVI observations was 0.68, and was identical at all scales from 1.5 to 9.0 m (Table 3), and very similar to the median values. The mean NDVI estimated for the same range of scales using individual, coarser samplings (Table 1) was larger, 0.73, but also did not vary across the pixel resolution from 1.5 to 9.0 m (Table 3). Again, the median values were very similar (0.74). NDVI generated by averaging the finest resolution data (0.2 m) plotted against single observations at increasingly coarser resolution showed a strong linear relationship across the range of scales (Fig. 2). The slopes and intercepts of the linear regressions fitted to the NDVI comparisons were very similar in all cases.

**Microscale LAI.** The fine scale estimates of LAI (0.2 m resolution), derived from co-located Skye NDVI and LAI-2000 observations, were aggregated at various scales (1.5–9.0 m resolution) and compared with

**Table 2** Testing different techniques of LAI extrapolation

Technique	Ground	Landsat	RMSE	MAE
	LAI	NDVI		
Inverse distance weighting (IDW)	Yes	No	0.27	0.21
Linear correlation model (LCM)	Yes	Yes	0.28	0.21
Ordinary Kriging (OK)	Yes	No	0.28	0.21
External drift Kriging (EDK)	Yes	Yes	0.29	0.22

All techniques used ground leaf area index (LAI) estimates, but only some used Landsat NDVI data. Root-mean-square error (RMSE) and mean absolute error (MAE) of the jackknife test are shown.

**Table 3** Comparison of Skye NDVI generated across a range of scales in the microscale plots

Resolution (m)	1.5		3.0		4.5		6.0		9.0	
No. of observations per pixel ( <i>n</i> )	6	1	25	1	69	1	125	1	625	1
No. of replicates ( <i>n'</i> )	900		225		81		45		9	
Minimum	0.36	0.50	0.47	0.56	0.51	0.61	0.53	0.62	0.59	0.67
Median	0.69	0.75	0.69	0.74	0.68	0.73	0.68	0.73	0.68	0.74
Maximum	0.83	0.85	0.80	0.83	0.79	0.80	0.78	0.83	0.76	0.78
Mean	0.68	0.73	0.68	0.73	0.68	0.73	0.68	0.73	0.68	0.73
Standard deviation	0.080	0.061	0.070	0.054	0.062	0.047	0.055	0.046	0.052	0.04
Variance	0.0063	0.0037	0.0049	0.0029	0.0039	0.0022	0.0031	0.0021	0.0027	0.0015
Skewness	-0.95	-0.89	-0.72	-0.85	-0.55	-0.88	-0.29	-0.27	-0.29	-0.29
Kurtosis	3.73	3.62	3.15	3.42	3.06	3.21	2.74	2.52	2.30	1.75

At each pixel resolution, there are two methods for determination of NDVI, classified by whether the NDVI is the average of several fine-scale NDVI measurements ( $n > 1$ ), or is determined by a single measurement ( $n = 1$ ). The number of replicates ( $n'$ ) indicates the number of pixels at each resolution, which are then used to generate statistics of NDVI at different scales and generated with different numbers of observations ( $n$ ), in the columns above.

corresponding single Skye NDVI estimates at those scales (Fig. 3). A simple exponential fit of NDVI–LAI using maximum likelihood approaches with an assessment of LAI estimation error (Van Wijk & Williams, 2005) was successful (i.e. acceptable parameter combinations were identified,  $P < 0.05$ ) at each scale of comparison (Fig. 3). This successful fit was in contrast to the case at  $0.2\text{ m} \times 0.2\text{ m}$  reported in Van Wijk & Williams (2005), which required the combination of Skye NDVI and LAI-2000 data to generate an acceptable estimation of LAI. The exponential fits are able to explain 80–94% of the variability in LAI from NDVI data. The parameters for the exponential relationships were similar across all scales (Fig. 3). The RMSE of the LAI–NDVI relationships varied from 0.18 at 1.5 m resolution to 0.08 at 9.0 m resolution (Fig. 3). As the range of LAI and NDVI variability declined with coarsening resolution, linear fits became increasingly acceptable, although the exponential models were always better.

The mean LAI for the microscale site generated using 0.2 m resolution data was 0.69, and the median was 0.65. Both the NDVI data (Table 3) and the LAI estimates derived from NDVI and LAI-2000 (Fig. 4) show decreasing ranges with spatial aggregation. At the finest scales, some sites had LAI values very close to zero, but the minimum LAI ( $L_{\min}$ ) estimate increased linearly with resolution, ( $L_{\min} = 0.0371r - 0.0108$ , where  $r$  is resolution in metres,  $R^2 = 0.99$ ,  $n = 6$ ). The maximum LAI dropped sharply in the aggregation from 0.2 m (max = 3.68) to 1.5 m (max = 1.75), but thereafter declined slowly. The distribution of LAI at 0.2 m resolution was highly skewed, but tended towards normality at coarser aggregations (Fig. 4).

*Spatial autocorrelation.* There was clear spatial autocorrelation in the microscale estimates of LAI, as indicated in the semivariogram (Fig. 5). However, the autocorrelation dropped rapidly at distances beyond 1.2 m. A more gentle decline followed, with the sill value reaching at 8 m. The discontinuity at the origin of the semivariogram (the ‘nugget’) is a combination of noise and the interaction of the discrete nature of plants with the sampling scale. So the nugget represents a fundamental uncertainty in observed LAI. The nugget value of 0.03 suggested that the standard deviation on LAI uncertainty was 0.17 ( $0.03^{0.5}$ ).

#### Macroscale study

*Macroscale NDVI and LAI.* The mean NDVI recorded across the 197 tundra sample locations at a resolution of 9 m was 0.75, close to the mean value of 0.73 recorded using the same sampling approach at the microscale site (Table 3). The distribution of measured NDVI was skewed towards higher values (Fig. 6). Using the relationship between LAI and NDVI generated using microscale data at 9 m resolution (Fig. 3), LAI was estimated for all macroscale locations. The mean estimated LAI was 0.84 with a range from 0.14 to 1.60, and a distribution without skew (Fig. 6), similar to the distributions of LAI determined at  $\geq 3$  m resolution in the microscale study (Fig. 4). We tested deriving macroscale LAI estimates using the LAI–NDVI relationships from the other microscale resolutions, 1.5–6.0 m (Fig. 3). The mean LAI ( $n = 197$ ) using all relationships was 0.82, and the individual relationships differed from the mean by 1–7%, so there is little difference between the relationships.

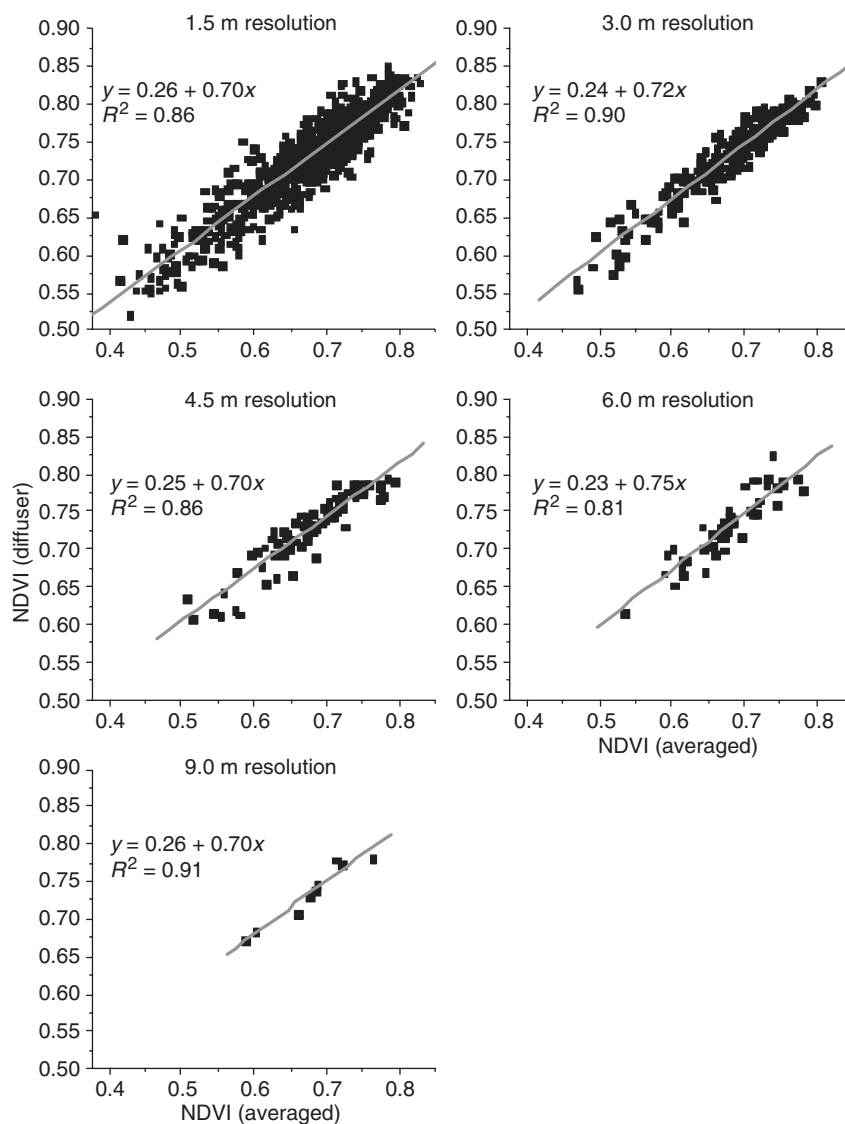


**Fig. 2** Linear averaged Skye NDVIs (collected at  $0.2\text{ m} \times 0.2\text{ m}$  resolution with diffuser off) vs. measured NDVIs at coarser spatial scales with diffuser on. Linear regression equations and  $R^2$ -values are shown.

The NDVI estimated by airborne sampling of the entire macroscale area was 0.74, close to the mean value of the macroscale field measurements. Using the upscaled NDVI–LAI relationship (Fig. 3) resulted in estimate of LAI of 0.70 at 700 m resolution for the IV, 17% less than the estimate summed from 9 m resolution ground data. This error is what might be expected, given the RMSE of the LAI–NDVI relationship from the microscale study.

*Macroscale geostatistics.* Semivariograms for the macroscale observations of LAI and NDVI in the IV, and also the Landsat observations of NDVI for the same locations, indicated clear spatial autocorrelation (Fig. 7).

Pairs of data observations separated by  $<160\text{ m}$  showed clear autocorrelation in both analyses. The sill values (i.e. maximum semivariance) for the satellite NDVI analysis were larger than those for the ground-based NDVI, and this was likely due to the effect of atmospheric interference and differences in viewing angle (Lillesand *et al.*, 2003). The nugget value was 50% greater for the Skye NDVI than for the Landsat data, but the ground-based values require less extrapolation and thus are more trustworthy. The nugget on the macroscale semivariogram was the same as that determined on the microscale data, again indicating an uncertainty in LAI estimates of 0.17. At distances of 50 m, the standard deviation in LAI increased by  $>50\%$  to 0.26.

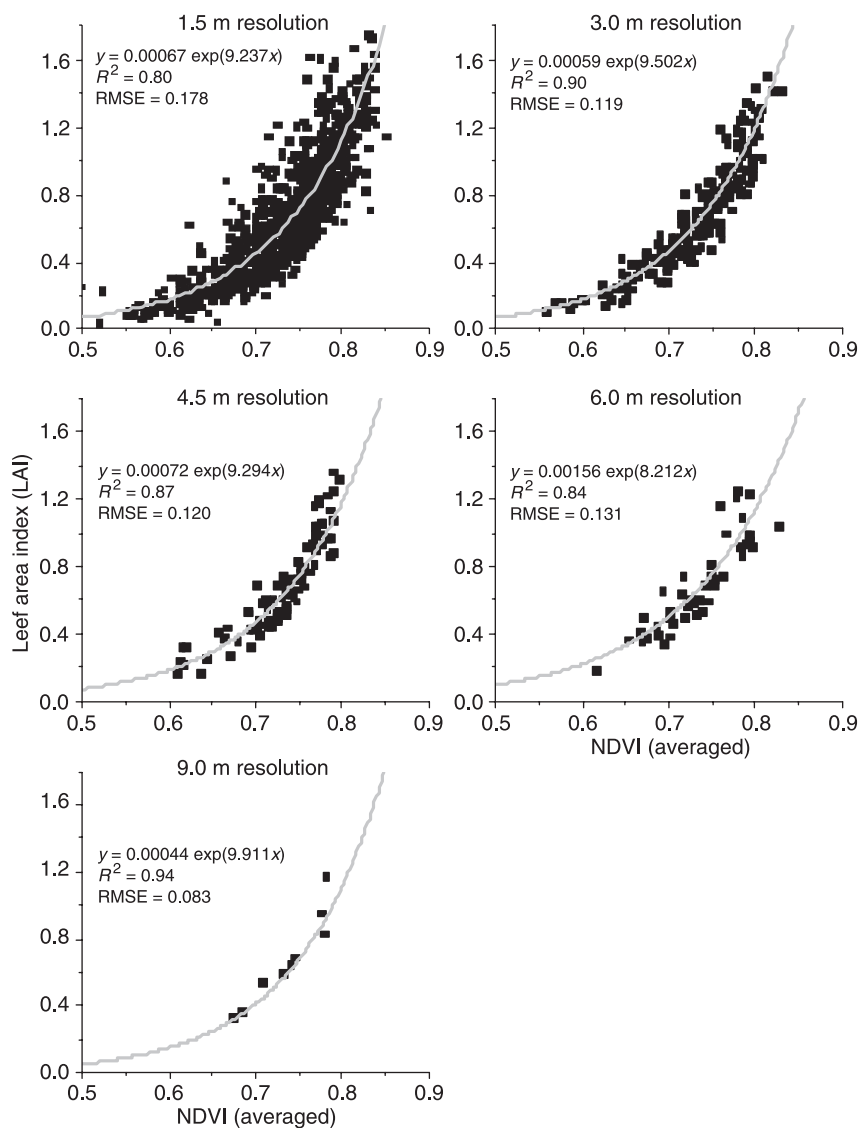


**Fig. 3** Relationships between estimated LAI (using both Skye NDVI and LI-COR LAI-2000 observations at 0.2 m resolution, linearly averaged for upscaling) vs. Skye NDVI at different spatial scales. Exponential model equations,  $R^2$ , and root-mean-square error are shown.

*Satellite data.* The comparison of ground-based NDVI with Landsat NDVI revealed a highly significant linear relationship (Fig. 8,  $r^2 = 0.20$ ,  $P < 0.0001$ ). The intercept was not significantly different from zero ( $P = 0.446$ ) but the slope of the relationship (0.55) was significantly different from one ( $P < 0.001$ ). A simple linear correlation model (LCM) between Landsat NDVI and ground-based LAI at the macroscale sites was developed ( $R^2 = 0.17$ ,  $\text{LAI} = -0.004 + 2.1 \text{ NDVI}$ , data not shown). The LCM predictions of LAI had an RMSE of 0.28 for the macroscale plots. Semivariograms of NDVI from Skye and Landsat showed a very similar form (Fig. 7), suggesting a detection of the same underlying spatial pattern. However, the frequency distribution of Landsat NDVI values was quite

different to Skye NDVI measurements (Fig. 6). The satellite data showed a peak in frequency towards the low end of the measurement range, while the ground data showed a peak towards the high end of the range.

*Extrapolation of LAI.* Extrapolation with the linear correlation model (LCM, Fig. 9), inverse distance weighting (IDW), ordinary Kriging (OK, not shown) and External Drift Kriging (EDK), generated maps with some clear commonalities, but also differences. All approaches predicted an increase in LAI towards the north of the IV, matching the local drop in elevation. There was a smoother LAI distribution with IDW and OK compared with LCM and EDK.

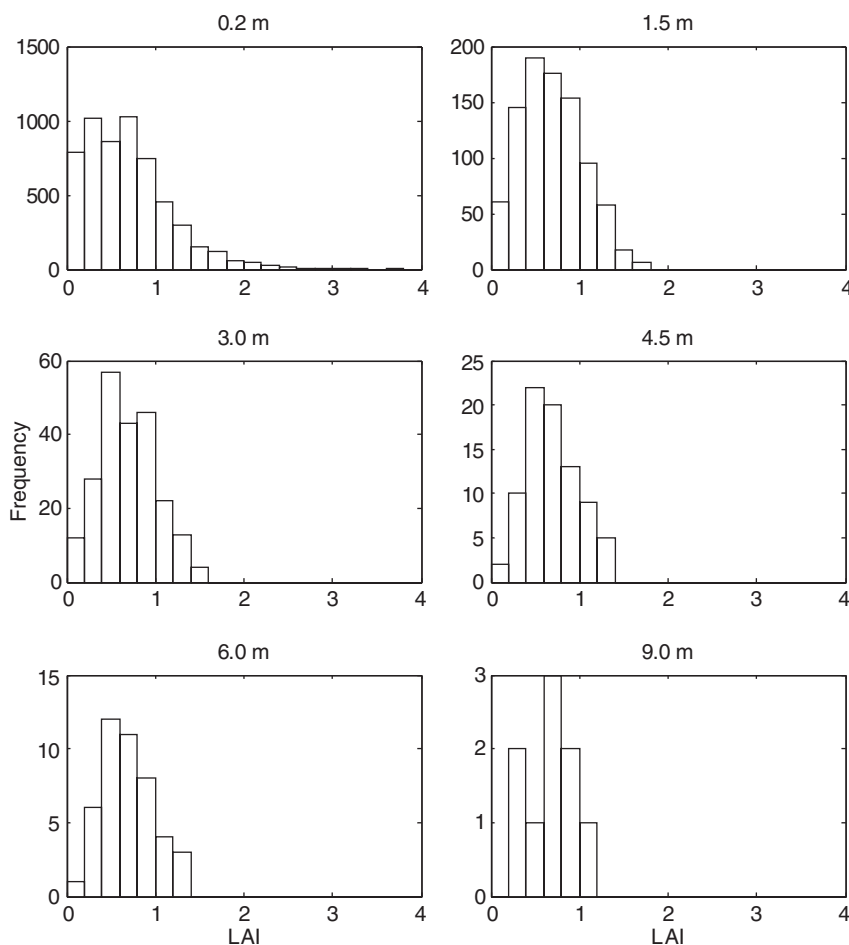


**Fig. 4** Frequency histograms for LAI estimates in the microscale site at a range of resolutions. LAI was derived from the calibrated NDVI and LAI-2000 relationship at 0.2 m resolution. The complete 5625 estimates are shown in the top left panel. In succeeding panels, the data are aggregated into coarser pixels by linear averaging.

The four methods showed similar overall skill, as determined in the jackknifing of predicted LAI against LAI estimates from Skye NDVI (Table 2). These techniques make use of different datasets and assumptions, so this similarity is unexpected. The Kriging methods have the advantage of producing spatial error estimates, which clearly were minimized around ground sampling points, and maximized in areas with sparse sampling (Fig. 9, lower right panel). Some ground sampling points were left out if there was tree cover, and this explains some of the largest concentrations of error. In Kriging, the growth of error with distance from ground sampling points is determined by the semivariograms (Fig. 7).

## Discussion

### *Comparing NDVI measurements across scales*

The microscale multiresolution data were consistent with the hypothesis (H1) that NDVI averaged linearly

at resolutions from 0.2 to 9.0 m (Fig. 2). The coarse measurements of NDVI were slightly offset from the finescale averages, probably due to the presence of the cosine diffuser on the sensor during the coarse measurements. However, at all scales of averaging up to 9 m, the linear regression parameters were very similar. These sensor resolutions are estimates only, because the instrumental field of view does not have sharp boundaries, but rather a weighting towards  $113^\circ$ . Furthermore, there was some error associated with the location of each sensor reading, particularly those where the sensor was suspended over the land-surface at heights of 2 or 3 m. The landscape is heterogeneous, with a highly skewed distribution in NDVI at fine (0.2 m) scales. Nevertheless, the results here show that single, coarse pixel measurements capture the mean properties of surface reflectance accurately. The lack of falsification for H1 is a powerful support for the subsequent scaling exercises.

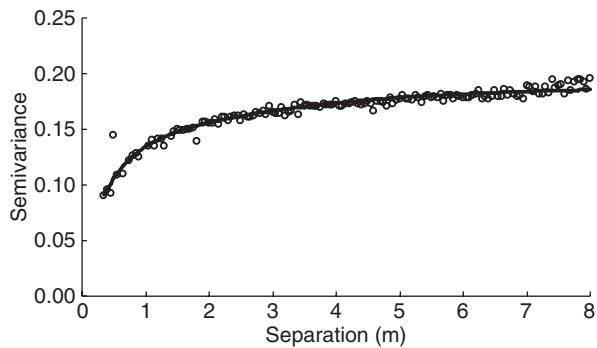


**Fig. 5** Semivariogram for LAI in the microscale study. The plot demonstrates the increase in spatial variance with separation distance using all paired measurements from 5625 LAI estimates (symbols). An exponential model (solid line) is fitted to the observations. The nugget variance is 0.03, the range for the first exponential model is 1.2 m, and for the second is 8.0 m, where the sill is 0.19.

#### *Scale invariance in LAI–NDVI relationships*

In support of hypothesis (H2), we found that LAI–NDVI relationships were scale-invariant in the microscale study (Fig. 3). At all resolutions, from 1.5 to 9.0 m, a simple exponential relationship linked upscaled LAI with Skye NDVI measured directly at the relevant resolution. While these LAI–NDVI relationships were all similar (in terms of parameters), they differed from the LAI–NDVI relationship at 0.2 m (Van Wijk & Williams, 2005), because the 0.2 m resolution data were collected without a diffuser. More importantly, the coarse scale LAI–NDVI relationships were all stronger ( $0.80 < R^2 > 0.94$ ) compared with the original study at 0.2 m ( $R^2 = 0.73$ ) and outputs from the relationships differed by only a few percent. Further, maximum likelihood analyses (Van Wijk & Williams, 2005) undertaken on the data from this study indicated that the NDVI data alone were able to provide a satisfactory prediction of LAI at resolutions from 1.5 to 9.0 m, which was not the case for 0.2 m resolution data. This improvement in the capabilities of NDVI as a predictor of LAI is likely to be due to the averaging of LAI values occurring at coarser resolutions. NDVI performed poorly in estimating higher LAI values at 0.2 m resolution, but maximum LAI dropped sharply with scale aggregation (Fig. 4) so this problem was negated.

The outcome of this hypothesis testing is that carefully calibrated LAI estimates developed at 0.2 m using destructive harvests have been used to develop a robust calibration of LAI–NDVI at a range of coarse resolutions which approach those typical of aircraft and satellite remote sensing. The error properties of the LAI–NDVI relationship are well characterized. As far as we know,

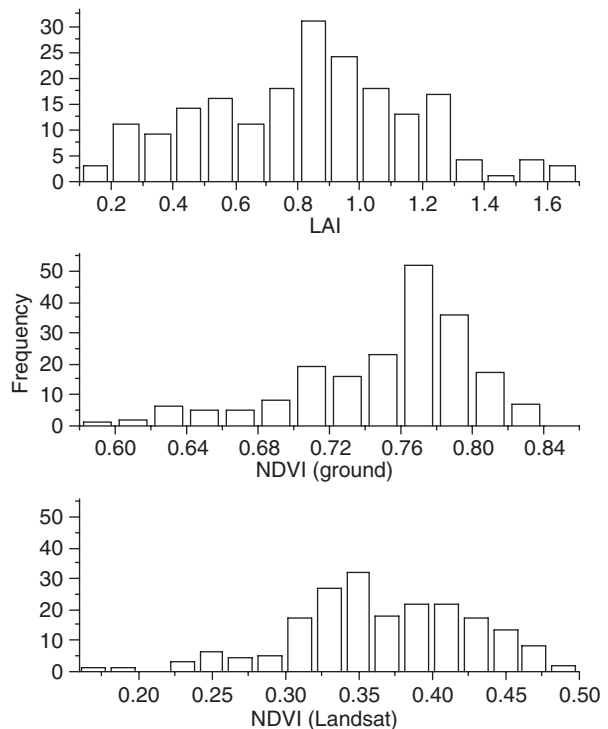


**Fig. 6** Histograms showing the variation in NDVI/LAI recorded in the macroscale study, at the 197 tundra sampling points (Fig. 1). The panels show a comparison between Landsat ETM+ NDVI data (lower panel), NDVI recorded in the field at 9 m resolution (middle panel), and LAI (upper panel) estimated using the 9 m resolution data using the equation from Fig. 3.

this study is the first to link direct measurements of canopy structure (i.e. LAI) at fine scales to remote sensing data with replication across scales spanning more than an order of magnitude.

#### *Spatial distribution of LAI*

We hypothesized (H3) that the range of LAI data estimated for a sample area would decline with a coarser sampling, and that the distribution of estimated LAI would be increasingly skewed at finer measurement scales. We found clear shifts in probability density functions for LAI in the microscale study, with increasingly skewed distributions at finer scales (Fig. 4). Spatial autocorrelation of LAI in the microscale study was greatest at  $< 1$  m separation (Fig. 5), indicating that  $\sim 0.5$  m was the approximate scale of vegetation patches. In accordance with this analysis, the greatest variation in NDVI and LAI was at the finest scale of sampling (0.2 m), while the range of both NDVI and LAI dropped rapidly at more aggregated scales. It is interesting that the LAI semivariogram for the macroscale study has similar nugget values to the microscale

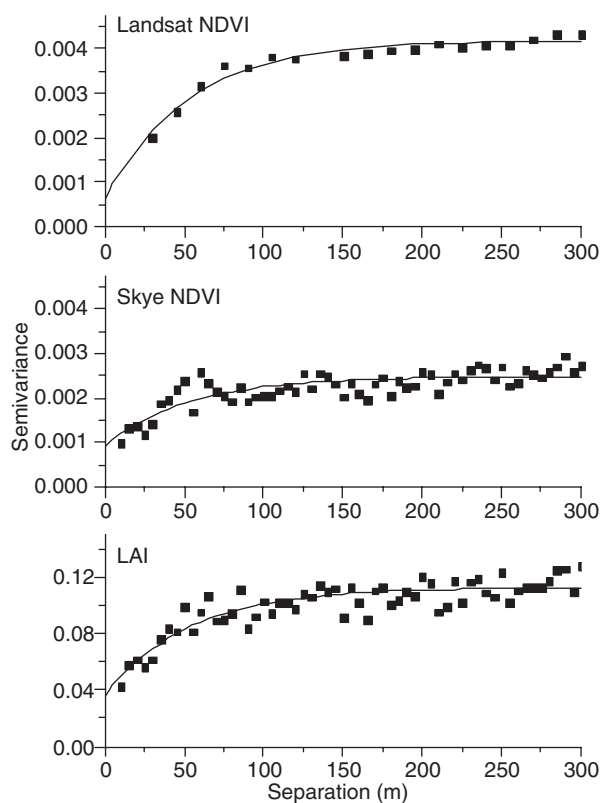


**Fig. 7** Semivariograms for LAI and NDVI in the macroscale study of the intensive valley. The middle panel was generated from Skye NDVI, and the lower panel from associated estimates of LAI. The top panel was generated from Landsat NDVI for the same locations. Exponential models (solid lines) are fitted to the observations (symbols).

semivariogram, but sill values in the macroscale study are around half those in the microscale study. This comparison suggests that at coarser scales of measurement, the variance of canopy characteristics declines as the values of extreme, small patches are subsumed.

The quality of autocorrelation statistics depends on the quality of the datasets used to generate them, so their results must be interpreted cautiously. We used very simple geostatistical models, taking no account of topography, which is likely to be an important factor in controlling the distribution of vegetation.

#### *Assessing LAI with satellite NDVI data*

Our first objective was to test the quality of space-borne observations of NDVI against ground data. The comparison of ground estimated LAI vs. Landsat NDVI was poor (though significant), with relatively large prediction errors (Fig. 8). Partly, this error may be due to the different wavebands sampled by the ground and Landsat sensors. It is possible that georeferencing errors have

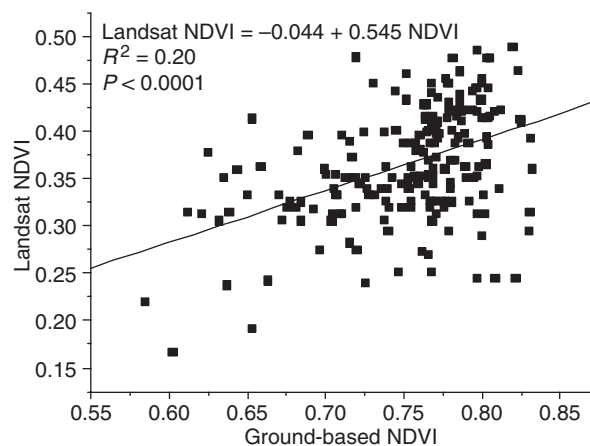


**Fig. 8** A comparison across the macroscale area of the intensive valley of ground-based NDVI using 9 m resolution measurements and Landsat NDVI measurements for the same locations. The line indicates the linear regression. Note that Landsat NDVI and ground-based NDVI sample different wavebands, and atmospheric corrections have not been undertaken.

degraded the correlation in our study, but such errors are inherent in most satellite remote sensing studies. The comparison of histograms of Skye and Landsat NDVI (Fig. 6) show that there are clear differences between the landscape signals, that are unlikely to be explained by spatial errors of  $\sim 6$  m from the GPS. Other comparisons of Landsat NDVI vs. LAI have shown similar, poor correlations for temperate and boreal ecosystems (Lee *et al.*, 2004). A comparison of 1 km AVHRR NDVI vs. LAI from tundra in the Alaskan Arctic had a similar, weak correlation coefficient (Williams *et al.*, 2001). Lee *et al.* (2004) concluded that satellite NDVI was generally not sensitive to LAI. Our ground-based studies have shown that this is not the case, because Skye NDVI was highly sensitive to LAI. There was a poor correlation between Skye NDVI and Landsat NDVI data, and so it seems that errors in the satellite data cause the relationship observed at ground level to break down.

The poor Skye vs. Landsat NDVI correlation and large offset of the satellite data reflects several uncertainties. Firstly, there were georeferencing errors in both the ground-based and satellite data. We explored these errors by introducing 7 m buffer zones into the ground data locations, corresponding to the GPS error. For the buffer zone around each Skye NDVI measurement, we determined the mean NDVI of all underlying Landsat pixels. The result was only a small improvement in the NDVI–NDVI correlation coefficient (data not shown) suggesting that small uncertainties in the handheld GPS and spatial uncertainty introduced by raising the sensor height were not the cause of the poor relationship.

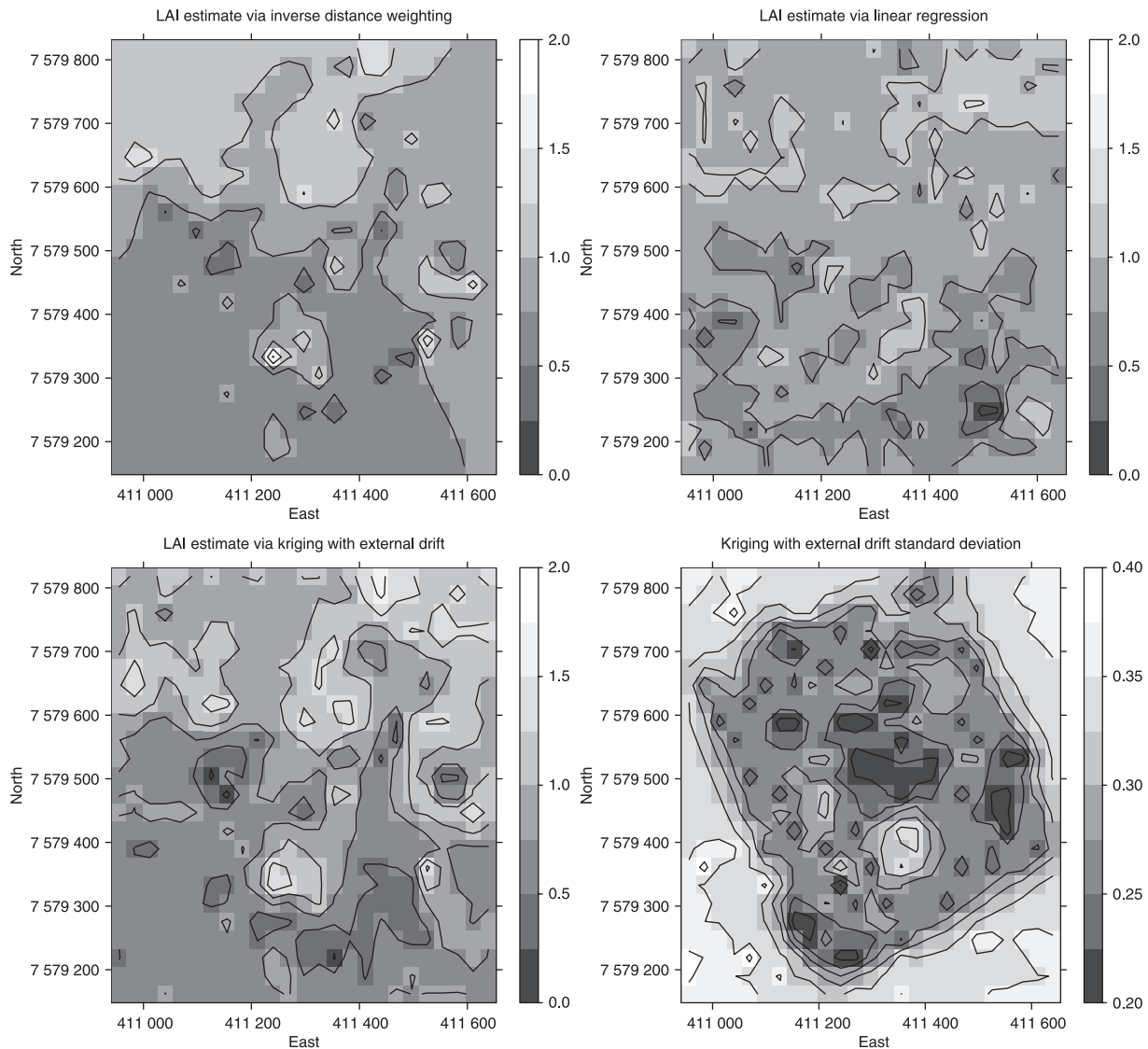


**Fig. 9** Maps of LAI for the intensive valley for late August, using inverse distance weighting of ground-based NDVI data (upper left); a simple correlation model of ground-based LAI vs. Landsat NDVI data (upper right); Kriging of ground-based NDVI data with external drift from Landsat NDVI data (lower left). The error associated with the Kriging are shown in the lower right panel. Contour lines are overlaid on the pixels. The units of the axes are in metres, based on a UTM coordinate system.

Secondly, there were errors related to the temporal offset in NDVI collection. The Landsat data were from late August 2001, and the macroscale data were collected in late August 2004. Phenological differences between years are possible. Finally, there were errors introduced by differences between sensor optics, sampled wavebands, atmospheric attenuation of signals, and local illumination conditions (Alter-Gartenberg *et al.*, 2002) to be considered. Atmospheric correction of the reflectance data could improve the estimate of NDVI, but the required atmospheric data were not available. Future studies should combine ground-based and airborne remote sensing with the

necessary atmospheric transmissivity corrections and should use the same wavebands to reduce uncertainties in NDVI/LAI estimation at larger spatial scales.

#### *Maps of LAI, and estimation errors*

Our second objective was to generate maps of LAI across the macroscale site, using a variety of approaches with remote sensing data and geostatistics. We hypothesized (H4) that geostatistical interpolations of ground data combined with remotely sensed NDVI data, through Kriging, would produce better maps than either interpolation or satellite-based approaches alone,

but our results showed this was not clear cut. All four approaches produced roughly the same level of mean estimation error (Table 2). We found that ground-based NDVI data were excellent at generating local LAI estimates, with mean estimation errors of typically 0.08–0.17. However, spatial autocorrelation dropped rapidly with increasing separation, so that at <50 m separation, LAI errors were typically  $\sim 0.3$ . The LCM between Landsat NDVI and ground estimates of LAI had an RMSE of 0.28. The similarity in magnitude of the spatial error and the Landsat calibration error accounts for the similarity in prediction capability across the macroscale area. Of course, around the ground measurement locations the prediction error was smaller, and so methods like Kriging have the advantage of reducing prediction error wherever extra data are available (Fig. 9). But the spatial variability of this Arctic landscape is such that local measurements have a limited spatial influence.

#### *Spatial data assimilation*

The assimilation of multiple data sources requires a careful determination of data error, so that data can be suitably weighted to produce an analysis. DA approaches are now being used commonly in ecological research to generate state estimates, by combining process information with multiple data series (Raupach *et al.*, 2005; Williams *et al.*, 2005). These techniques are now being used to assimilate remote sensing data sequentially into ecosystem models (Quaife *et al.*, 2008). For such time-series DA approaches to be applied across regions or globally, spatial assimilation approaches such as Kriging become important tools for generating estimates of initial conditions in state variables, and for generating spatial errors. There is an urgent need to develop a closely coupled spatio-temporal assimilation system. This system would combine the strengths of time-series analysis with geostatistical approaches, to simulate ecological processes, and more effectively link networks of field sites – with high resolution process data – with global, repeated reflectance data from Earth Observation systems.

#### **Conclusions**

With multiple nested reflectance measurements on an Arctic tundra, we showed that NDVI scaled linearly with increasing spatial grain, and that the LAI–NDVI relationship was scale invariant from 1.5 to 9.0 m resolution. Thus, a single exponential LAI–NDVI relationship was valid at all scales, with similar prediction errors. An analysis of semivariograms showed that vegetation patches were of a scale of  $\sim 0.5$  m, and at

measurement scales coarser than this there was a sharp drop in LAI variance. Landsat NDVI data for the study catchment correlated significantly, but weakly, with ground-based NDVI measurements. A variety of techniques were used to construct LAI maps across the catchment, including interpolation by IDW, OK, EDK using Landsat data, and direct estimation from the Landsat NDVI–LAI calibration. All four methods produced similar estimates of LAI and errors of similar magnitude. The Kriging approaches also generated maps of LAI estimation error based on semivariograms. The spatial variability of this Arctic landscape was such that local measurements assimilated by Kriging approaches had a limited spatial influence. Over scales > 50 m interpolation error was of similar magnitude to the uncertainty in the Landsat NDVI calibration to LAI. The characterisation of LAI errors in this study (Fig. 3 and Table 2) is a key step towards developing spatio-temporal DA systems for assessing C cycling in Arctic ecosystems from combining models, field and remotely sensed data sources.

#### **Acknowledgements**

We acknowledge funding from the US National Science Foundation (Grant nos. OPP-0096523, OPP-0352897, DEB-0087046, and DEB-00895825), from the University of Edinburgh, and from the Natural Environment Research Council. We thank Sven Rasmussen for field assistance, and Terry Callaghan for the support and facilities of the Abisko Research Station, and Paul Stoy for his comments on the manuscript.

#### **References**

- Alter-Gartenberg R, Nolf SR, Davis RE (2002) A sensitivity assessment of terrestrial identification in remote sensing. *International Journal of Remote Sensing*, **23**, 825–849.
- Anderson NA, Callaghan TV, Karlsson PS (1996) The Abisko Scientific Research Station in plant ecology in the subarctic Swedish Lapland (eds Karlsson PS, Callaghan TV). *Ecological Bulletins*, **45**, 11–14.
- Boelman NT, Stieglitz M, Griffin KL, Shaver GR (2005) Inter-annual variability of NDVI in response to long-term warming and fertilization in wet sedge and tussock tundra. *Oecologia*, **143**, 588–597.
- Boelman NT, Stieglitz M, Rueth HM, Sommerkorn M, Griffin KL, Shaver GR, Gamon JA (2003) Response of NDVI, biomass, and ecosystem gas exchange to long-term warming and fertilization in wet sedge tundra. *Oecologia*, **135**, 414–421.
- Callaghan TV, Karlsson PS (1996) Plant ecology in the Swedish Lapland: summary and conclusions. *Ecological Bulletins*, **45**, 220–227.
- Chapin FS III, Sturm M, Serreze MC *et al.* (2005) Role of land-surface changes in Arctic summer warming. *Science*, **310**, 657–660.
- Cressie NAC (1993) *Statistics for Spatial Data*, revised edn. Wiley, New York.

- Deutsch CV, Journel AG (1998) *GSLIB: Geostatistical Software Library and Users Guide*, 2nd edn. Oxford University Press, New York.
- Essery R, Best M, Cox P (2001) *MOSES 2.2 Technical Documentation, Rep. No. HCTN 30*. UK Met Office, Bracknell, UK.
- Goovaerts P (1999) Geostatistics in soil science: state-of-the-art and perspectives. *Geoderma*, **89**, 1–45.
- Harvey LDD (2000) Upscaling in global change research. *Climatic Change*, **44**, 225–263.
- Isaaks EH, Srivastava RM (1990) *Applied Geostatistics*. Oxford University Press, Oxford.
- Jia GS, Epstein HE, Walker DA (2006) Spatial heterogeneity of tundra vegetation response to recent temperature changes. *Global Change Biology*, **12**, 42–55.
- Lee KS, Cohen WB, Kennedy RE, Maieringer TK (2004) Hyperspectral versus multispectral data for estimating leaf area index in four different biomes. *Remote Sensing of Environment*, **91**, 508–520.
- Lillesand TM, Kiefer RW, Chipman JW (2003) *Remote Sensing and Image Interpretation*, 5th edn. Wiley, Chichester, UK.
- Myneni RB, Keeling CD, Tucker CJ, Asrar G, Nemani RR (1997) Increased plant growth in the northern high latitudes from 1981–1991. *Nature*, **386**, 698–702.
- Owen KE, Tenhunen J, Reichstein M *et al.* (2007) Linking flux network measurements to continental scale simulations: ecosystem carbon dioxide exchange capacity under non-water-stressed conditions. *Global Change Biology*, **13**, 734–760.
- Quaife T, Lewis P, De Kauwe M, Williams M, Law BE, Disney M, Bowyer P (2008) Assimilating canopy reflectance data into an ecosystem model with an ensemble Kalman filter. *Remote Sensing of the Environment*, **112**, 1347–1364.
- Raupach MR, Rayner PJ, Barrett DJ *et al.* (2005) Model-data synthesis in terrestrial carbon observation: methods, data requirements and data uncertainty specifications. *Global Change Biology*, **11**, 378–397.
- Sitch S, Smith B, Prentice IC *et al.* (2003) Evaluation of ecosystem dynamics, plant geography and terrestrial carbon cycling in the LPJ dynamic global vegetation model. *Global Change Biology*, **9**, 161–185.
- Street LE, Shaver GR, Williams M, Van Wijk MT (2007) What is the relationship between changes in canopy leaf area and changes in photosynthetic CO<sub>2</sub> flux in arctic ecosystems. *Journal of Ecology*, **95**, 139–150.
- Tian YH, Woodcock CE, Wang YJ *et al.* (2002) Multiscale analysis and validation of the MODIS LAI product – I Uncertainty assessment. *Remote Sensing of Environment*, **83**, 414–430.
- Tucker CJ, Grant DM, Dykstra JD (2004) NASA's global orthorectified Landsat data set. *Photogrammetric Engineering and Remote Sensing*, **70**, 313–322.
- Turner DP, Cohen WB, Kennedy RE, Fassnacht KS (1999) Relationships between leaf area index and Landsat TM spectral vegetation indices across three temperate zone sites. *Remote Sensing of Environment*, **70**, 52–68.
- Van Wijk MT, Williams M (2005) Optical instruments for measuring leaf area index in low vegetation: application in arctic ecosystems. *Ecological Applications*, **15**, 1462–1470.
- Williams M, Rastetter EB (1999) Vegetation characteristics and primary productivity along an arctic transect: implications for scaling-up. *Journal of Ecology*, **87**, 885–898.
- Williams M, Rastetter EB, Shaver GR, Hobbie JE, Carpino E, Kwiatkowski BL (2001) Primary production in an arctic watershed: an uncertainty analysis. *Ecological Applications*, **11**, 1800–1816.
- Williams M, Schwarz P, Law BE, Irvine J, Kurpius MR (2005) An improved analysis of forest carbon dynamics using data assimilation. *Global Change Biology*, **11**, 89–105.
- Woodcock CE, Strahler AH (1987) The factor of scale in remote sensing. *Remote Sensing of Environment*, **21**, 311–322.